

Simulation of the Performance of IEEE 802.16-2004 WirelessMAN-OFDM PHY

by

Mamatha Mannava

Problem report submitted to the
College of Engineering and Mineral Resources
at West Virginia University
in partial fulfillment of the requirements
for the degree of

Master of Science
in
Electrical Engineering

Matthew C.Valenti, Ph.D., Chair
Daryl Reynolds, Ph.D.,
Natalia A.Schmid, Ph.D.

Lane Department of Computer Science and Electrical Engineering

Morgantown, West Virginia
2008

Keywords: Broadband wireless access, WirelessMAN, OFDM, turbo codes

Copyright 2008 Mamatha Mannava

Abstract

Simulation of the Performance of IEEE 802.16-2004 WirelessMAN-OFDM PHY

by

Mamatha Mannava

Master of Science in Electrical Engineering

West Virginia University

Matthew C.Valenti, Ph.D., Chair

A revolution is about to occur in the broadband and wireless industries. These two industries, which have until now remained distinct, will soon merge with the deployment of broadband wireless access (BWA) technology. The leading candidate for BWA is WiMAX, a technology that complies with the IEEE 802.16 family of standards. In this report, we focus specifically on the WirelessMAN-OFDM physical layer of the IEEE 802.16-2004 standard, which uses a combination of quadrature amplitude modulation (QAM), orthogonal frequency division multiplexing (OFDM), and convolutional turbo coding (CTC). The contribution of the report is the derivation of a vector-based model for OFDM and its implementation in software. Using the software implementation, simulations were run showing the performance of the WirelessMAN-OFDM physical layer with a variety of link and channel configurations. The results show the effect of the code rate, modulation order, cyclic prefix length, and rms delay spread of the channel.

Acknowledgments

I am very grateful to Dr. Matthew Valenti for giving me this opportunity to do my problem report on one of the topics of the leading WiMAX technology. I am very happy to work on this topic. Research on this topic helped me enhance my knowledge and understanding. I would like to convey my sincere thanks to Dr. Matthew Valenti for agreeing to be my advisor and for helping me through in every tough situation. He is a very good advisor and a perfect professor to work with. I would also like to thank Dr. Daryl Reynolds and Dr. Natalia Schmid for being my committee members and for supporting me.

I would like to thank my husband Satya Kiran for supporting me in all aspects. I would have not made this possible without his help and support. Finally I would like to thank my friends, my dad M.Kishore Babu, my mother M.Sree Lakshmi and my sister Samatha. My family was of great support to me at all times.

Contents

Acknowledgments	iii
List of Figures	vi
1 Introduction	1
1.1 Objective	2
1.2 Structure of Report	2
2 IEEE 802.16 WiMax Overview	3
2.1 Overview of IEEE family	3
2.1.1 IEEE 802.16 2001	3
2.1.2 IEEE 802.16a-2003	4
2.1.3 IEEE 802.16c-2002	4
2.1.4 IEEE 802.16-2004	5
2.2 WiMAX forum and adaptation of IEEE 802.16	5
3 Orthogonal Frequency Division Multiplexing	6
3.1 WirelessMAN - OFDM PHY Layer	6
3.1.1 OFDM System Implementation	7
3.1.2 Cyclic Prefix	7
3.1.3 OFDM Design Considerations	9
3.1.4 Convolutional Turbo Coder (CTC)	10
3.2 Vector Model Implementation of OFDM	11
3.3 Benefits and Drawbacks of OFDM	13
4 Simulation Model	14
4.1 OFDM Symbol Parameters	14
4.2 Power Delay Profile (PDP) and RMS Delay Spread	17
4.2.1 Relation between rms delay spread, T_c and β	18
5 Results and Conclusion	20
5.1 Simulation Results	20
5.1.1 Influence of modulation type	20
5.1.2 Influence of CTC code rate	23
5.1.3 Influence of channel delay spread.	26
5.2 Conclusion	26

CONTENTS

v

References

29

List of Figures

3.1	OFDM Transmitter and Receiver with IFFT/FFT.	8
3.2	Cyclic Prefix addition and ISI between blocks in channel output	9
3.3	CTC encoder.	11
4.1	Allocation of the 256 subcarriers	15
4.2	OFDM subcarriers in frequency domain	16
4.3	Power delay profile as a function of time delay	18
5.1	BER vs. \mathcal{E}_s/N_0 of various modulations for fixed code rate of 1/2	21
5.2	BER vs. \mathcal{E}_b/N_0 of various modulations for fixed code rate of 1/2	22
5.3	FER vs. \mathcal{E}_s/N_0 of various modulations for fixed code rate of 1/2	22
5.4	FER vs. \mathcal{E}_b/N_0 of various modulations for fixed code rate of 1/2	23
5.5	BER vs. \mathcal{E}_s/N_0 of 64QAM modulation for various code rate	24
5.6	BER vs. \mathcal{E}_b/N_0 of 64QAM modulation for various code rate	24
5.7	FER vs. \mathcal{E}_s/N_0 of 64QAM modulation for various code rate	25
5.8	FER vs. \mathcal{E}_b/N_0 of 64QAM modulation for various code rate	25
5.9	BER vs. \mathcal{E}_s/N_0 of (48,24) QPSK modulation for various delay spread	26
5.10	BER vs. \mathcal{E}_b/N_0 of (48,24) QPSK modulation for various delay spread	27
5.11	FER vs. \mathcal{E}_s/N_0 of (48,24) QPSK modulation for various delay spread	27
5.12	FER vs. \mathcal{E}_b/N_0 of (48,24) QPSK modulation for various delay spread	28

Chapter 1

Introduction

WiMax stands for Worldwide Interoperability for Microwave Access. WiMax is now the leading broadband wireless access technology connecting remote locations and people in all areas. WiMAX technology has been standardized by the IEEE 802.16 working group, which has worked to overcome many of the limitations of other competing technologies. Cable and DSL have also tried to satisfy their customers by providing best access in all areas. But they failed due to some practical difficulties. Broadband wireless access (BWA) has overcome all these difficulties and provided customers with better access which is more flexible and efficient.

The number of Internet users is growing and the need for best Internet access is on demand. People use Internet for all purposes- downloading files, streaming various audio/video files and for transferring or receiving data. These are all regular day-to-day activities which require continuous broadband access and really satisfies users all over the world. IEEE 802.16 is one such standard prompted by the WiMax Forum to satisfy the need of users by offering high data rate and in turn higher bandwidth. WiMAX is based on OFDM technology with high-order QAM modulation and turbo coding. WiMax operates in different frequencies depending on the environment conditions. When operating in line of sight (LOS) conditions its frequency band is in range 10-66GHz and in non light of sight (NLOS) conditions it ranges from 2-11GHz. The IEEE 802.16 working group has come up with many standards by adding additional features to initial ones for better performance.

1.1 Objective

This main goal of this report is to implement, via simulation, the OFDM modulation used in the physical layer portion of the IEEE 802.16 standard. The main theoretical contribution is the development of a vector-based model for OFDM operating over frequency-selective fading channels. This model was implemented in matlab and integrated into the Coded Modulation Library (CML), an open source package for simulating digital communication systems. Using existing functions for encoding and decoding turbo codes, a set of simulations were run that demonstrate the performance of OFDM with turbo coding. The simulations were run under a variety of link and channel configurations, and results show the effect of the code rate, modulation order, cyclic-prefix size, and channel delay spread.

1.2 Structure of Report

The report is organized in five chapters. This first chapter has motivated the report and provided the objective. Chapter 2 gives an overview of the WiMAX Forum and the IEEE family of standards, focusing specifically on the IEEE 802.16 standard. Chapter 3 discusses in detail the OFDM PHY layer which includes the vector model representation and design considerations. A discussion is also provided on the topic of Convolutional Turbo Coding (CTC). Chapter 4 deals with the simulation model of OFDM followed by topics such as Power Delay Profile (PDP) and rms delay spread. The last chapter provides results obtained from the simulation of OFDM modulation and also concludes with a summary of the report and recommendation for future work.

Chapter 2

IEEE 802.16 WiMax Overview

This chapter first gives an overview of Wireless Metropolitan Area Network (WiMax) covering its related standards: 802.16-2001, 802.16a-2003 ,802.16c-2002 and then in detail 802.16-2004.

2.1 Overview of IEEE family

The IEEE Standard 802.16 family is known for its wireless access technology. Many standards have been developed over several years of hard work and research. WiMAX is now known for its Last Mile access technology which implies connecting people in every nook and corner to the Internet network. WiMAX gained popularity not only for its superior service but also for its low installation cost and easy maintenance.

2.1.1 IEEE 802.16 2001

The first member of the IEEE family of wireless metropolitan area networks (wireless MAN) is 802.16 2001 published in June 2002. This standard consists of MAC and PHY layers and works in the 10-66 GHz band under line of sight (LOS) conditions. This is the initial standard and the remaining standards are amendments to it. In the 10-66 GHz licensed frequency band, WiMax achieves data rates up to 120 Mbps. The standard offers point to multipoint wireless access and is based on single carrier modulation. The 802.16-2001 standard allows QPSK, 16QAM and 64QAM modulations. The standard also supports both

Time Division Duplexing (TDD) and Frequency Division Duplexing (FDD) techniques. The standard provides differential Quality of Service (QoS) in the MAC Layer. Single carrier modulation operated in frequency band 10-66GHz is also known as WirelessMAN-SC air interface.

2.1.2 IEEE 802.16a-2003

The standard IEEE 802.16a-2003 is an amendment to the first standard with improved features. This standard was developed in April 2003. The standard operates in licensed and unlicensed frequency band of 2-11 GHz in non light of sight (LOS) conditions where multipath propagation becomes a problem. NLOS condition is where LOS propagation is not likely. To overcome problems due to multipath propagation new features were required which were developed in 802.16a-2003. Features like advanced power management and adaptive antenna arrays were included in the standard. 802.16a standard supported three structures: single-carrier (SC) for line of sight condition, OFDM and OFDMA for non light of sight (NLOS) conditions. OFDM stands for Orthogonal Frequency Division Multiplexing and OFDMA stands for Orthogonal Frequency Division Multiple Access. The key difference between these OFDM and OFDMA is in the number of users using a channel. OFDM allows only single user to access a channel at any given time. By using TDMA and FDMA multiple users are allowed to access a channel at the same time. But this is not very efficient. So the problems due to multi users on a single channel are overcome by OFDMA. OFDMA allows multiple users to access a single channel at the same time. The maximum data rate supported by the standard is 75 Mbps. Security is made stronger in this specification and also changes have been made to some layers in previous standard. When making a comparison between the first and the second standards in frequency band, this standard has expanded its coverage.

2.1.3 IEEE 802.16c-2002

This standard is also an amendment to the first standard 802.16-2001. The published date of the standard is Jan 2003. This standard focused on system profiles, physical and data link

layers and also on errors and inconsistencies of the first standard.

2.1.4 IEEE 802.16-2004

IEEE 802.16 2004 standard is a collection of all the above three standards and is also a replacement to all the above. This standard is previously known as 802.16d. The new version was made active from July 2004. As this standard is used to address only fixed systems, systems using this standard are generally referred to as Fixed WiMax. Orthogonal frequency division multiplexing is used in this standard. Fixed and nomadic access is available in this standard. Modulations supported by this standard are 256-carrier OFDM and 2048-carrier OFDMA. WirelessMAN-OFDM which uses 256-carrier orthogonal frequency division multiplexing is discussed in later sections. Detailed discussion on Wireless MAN - OFDM PHY using this standard is made in next chapter.

2.2 WiMAX forum and adaptation of IEEE 802.16

The name WiMax was created by the WiMax Forum. The main purpose of the WiMAX forum is to create a set of profiles which specify the values of certain parameters selected from the IEEE 802.16 standard. The forum recognizes WiMax as a technology to enable and enhance the use of broadband wireless access as an replacement to wired Internet networks.

WiMax forum has developed two versions of the IEEE 802.16 standard to provide different types of access. They are Fixed or Nomadic access and Portable or Mobile access. IEEE 802.16-2004 standard is used for fixed or nomadic access. This provides support in both line of sight (LOS) and non line of sight (NLOS) conditions. The second version which is portable or mobile access is used by the IEEE 802.16e standard.

Chapter 3

Orthogonal Frequency Division Multiplexing

This chapter discusses the Wireless MAN-OFDM PHY layer with its specifications and conditions of operation. The OFDM system implementation and design parameters are overviewed. Details are provided regarding the convolutional turbo code (CTC) used in the physical layer. Finally the chapter concludes with a discussion of the vector model implementation of OFDM and the benefits and drawbacks of OFDM.

3.1 WirelessMAN - OFDM PHY Layer

OFDM is a type of multi-carrier modulation in which each symbol modulates one of a plurality of sub-carriers. The basic idea behind multi-carrier modulation is to transmit a single wideband signal by breaking it into N narrowband signals. This implies transmitting a signal with overall rate R over N subchannels each with rate R/N . If B_N denotes bandwidth of subchannel and B_c denotes the coherence bandwidth of the channel, then required is $B_N < B_c$, which implies each subchannel experiences flat fading. In 802.16-2004 standard, 256 point OFDM based air interface seems to gain popularity for reasons such as faster calculation of fast fourier transform (FFT), ability to withstand in difficult radio environment conditions, higher bandwidth efficiency, and less requirements for frequency synchronization when compared to Wireless MAN OFDMA. In 256 carrier OFDM, out of these 256 subcarri-

ers 192 are used data bits, 56 are nulled for guard band and 8 are used as pilot bits. OFDM is known for its higher bandwidth which in turn provides high data rates and robustness to noise. WirelessMAN OFDM system used here has FFT size N equal to 256.

3.1.1 OFDM System Implementation

In this report, the analysis for OFDM is based on a matrix representation of the system. The digital implementation of OFDM is obtained through operations such as Discrete Fourier Transform (DFT) and Inverse Discrete Fourier transform (IDFT). These two operations are used for transforming data between time and frequency domain. A discrete time equivalent low pass channel with finite impulse response (FIR) $h[n]$, $0 \leq n \leq \mu$ is considered along with input $x[n]$, noise $v[n]$, and output $y[n]$.

$$y[n] = x[n] \star h[n] + v[n] \quad (3.1)$$

Output $y[n]$ equals sum of two vectors- say vector 1 and vector 2. Vector 1 is the convolution of input $x[n]$ and impulse response $h[n]$ and vector 2 is just the noise $v[n]$. See equation 3.1. The n^{th} elements of the sequences are denoted as $h_n = h[n]$, $x_n = x[n]$, $v_n = v[n]$, and $y_n = y[n]$. A basic OFDM block diagram with IFFT/FFT is shown in Fig. 3.1.

In the matrix implementation of OFDM, for each OFDM symbol a vector \mathbf{h} is generated which contains complex valued path gains. Vector \mathbf{h} is a row vector of length $\mu + 1$. These complex valued path gains are independent complex gaussian random variables. The n^{th} variable in the \mathbf{h} vector, denoted h_n , is zero mean with power G_n . The relative power G is used to describe the power delay profile (PDP), which is discussed in next chapter.

3.1.2 Cyclic Prefix

Linear convolution between the channel input and impulse response can be turned into circular convolution by adding a special prefix to the input called a cyclic prefix (CP). Equation (3.1) gives the circular convolution in time domain. Circular convolution in the time domain corresponds to the multiplication of DFT's in the frequency domain. Therefore,

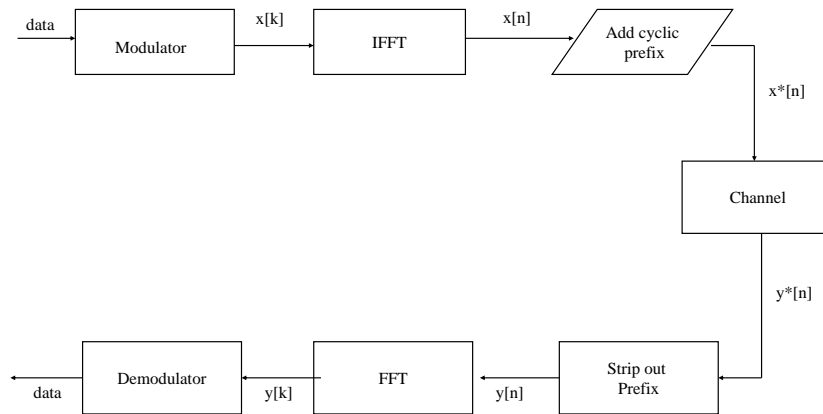


Figure 3.1: OFDM Transmitter and Receiver with IFFT/FFT.

(3.1) can be rewritten as:

$$Y[k] = X[k]H[k] + V[k] \quad (3.2)$$

where $X[k]$, $H[k]$, $V[k]$, and $Y[k]$ are the DFT's of $x[n]$, $h[n]$, $v[n]$, and $y[n]$, respectively.

The CP is used to remove ISI introduced by the multipath channel. CP is a copy of the last part of OFDM symbol which is appended to the front of transmitted OFDM symbol. This implies CP consists of last μ values of input sequence $x[n]$. Referring to Fig. 3.1, $x^*[n]$ is the signal with CP added. For each input sequence of length N , last μ samples are appended to the beginning to the sequence. Length of CP (T_g) is to be determined carefully. The length of the cyclic prefix should generally be chosen to match the maximum delay of the channel μ . For the remainder of this discussion we will assume that $T_g = \mu$. Fig. 3.2 illustrates the concept of cyclic prefix.

When a cyclic prefix is used, the length of the output becomes $N + \mu$. The first μ samples of $y^*[n]$ are not required to recover the input. $y^*[n]$ is the output signal with CP added. Due to the addition of the cyclic prefix, there occurs an overhead of μ/N resulting in data reduction of $N/(\mu + N)$. This results in loss of energy due to cyclic prefix and also pilots as

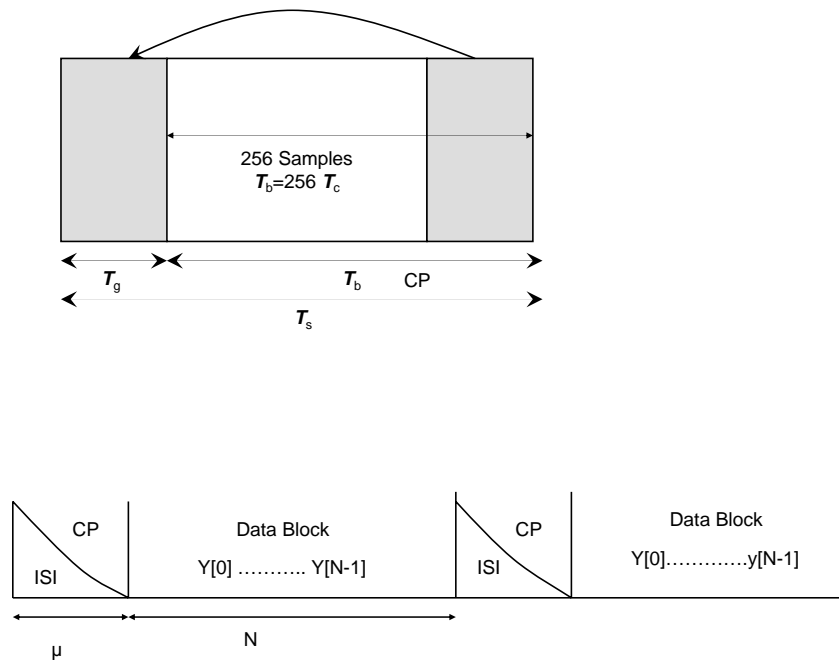


Figure 3.2: Cyclic Prefix addition and ISI between blocks in channel output

prefix consists of redundant data. Due to loss of energy, there occurs a shift of the \mathcal{E}_b/N_0 axis. The extent of the shift is determined by the ratio of energy used to send information. Say length T_g cyclic prefix requires an extra energy of T_g/N . For instance, if there are 192 data bits, 8 pilot symbols, and a cyclic prefix of length 64, then the ratio of energy used is $192/(192 + 8 + 64) = 3/4$. So \mathcal{E}_b/N_0 axis is to be shifted over by $10 \log(3/4) = -1.25$ dB.

3.1.3 OFDM Design Considerations

Main aim of OFDM design is to eliminate Inter Symbol Interference (ISI) and also to overcome multipath for best response and results. An increase in symbol duration results in a reduction of multipath effects. Choosing a longer cyclic prefix length is an effective way to eliminate the multipath effects but in turn increases loss of energy. Hence the choice of the cyclic prefix length is very important to obtain reasonable results.

Bandwidth, bit rate and delay spread play significant roles in determining system performance. In selection of subcarriers large bandwidth is preferred. RMS delay spread is determined by factors such as channel sample rate (T_c) and channel dependent parameter (β). The relationship between these three parameters is discussed in next chapter. Parameters such as bandwidth, number of used subcarriers, and sampling factor are not derived. A list of derived parameters are given below.

Derived Parameters

These parameters are derived according to system requirements. The following are the derived parameters. **Number of subcarriers (N_{FFT}):** large number of subcarriers helps reduce multipath effects but in turn increases complexity at receiver. **CP Time:** $T_g = GT_b$ where G is ratio of CP time to useful time. **Symbol Duration:** Ratio between CP length and symbol duration plays an important role. Good choice of this ratio prevents bandwidth loss due to CP. **Sampling Frequency:** F_s depend on bandwidth and sampling factor (n). **Subcarrier Spacing:** Spacing is determined by sampling frequency.

3.1.4 Convolutional Turbo Coder (CTC)

A convolutional code is a type of error-correcting code. Every encoded k bit symbol will be transformed into an n-bit symbol, where k/n is code rate for which ($n \leq k$). CTC is a type of turbo coding. Convolutional turbo coding is very significant in non LOS conditions. Use of convolutional turbo coding in OFDM improves the performance in many ways. A block diagram of CTC encoder is shown in Fig. 3.3. CTC encoder consists of two constituent encoders, an interleaver, and an optional puncturer. This system also consists of an on-off switch which operates accordingly. Encoder takes two input bits at one particular instance of time and output consists of 4 bits, two systematic and two parity bits. CTC encoder improves the performance of the system. Code words obtained are punctured to obtain the code rate by deleting certain parity bits. Typical data rate is 1/3 where for each data bit one systematic and two parity bits are produced. The rate can be increased by puncturing the data bits, but alternatively reducing the rate below 1/3 is very difficult. Convolutional

turbo coding is simple in implementation as it uses a single code for all frame sizes and code rates. The memory space required for CTC is also less when compared to Block codes. There are various patterns provided by standard in performing the puncturing task which are not discussed here.

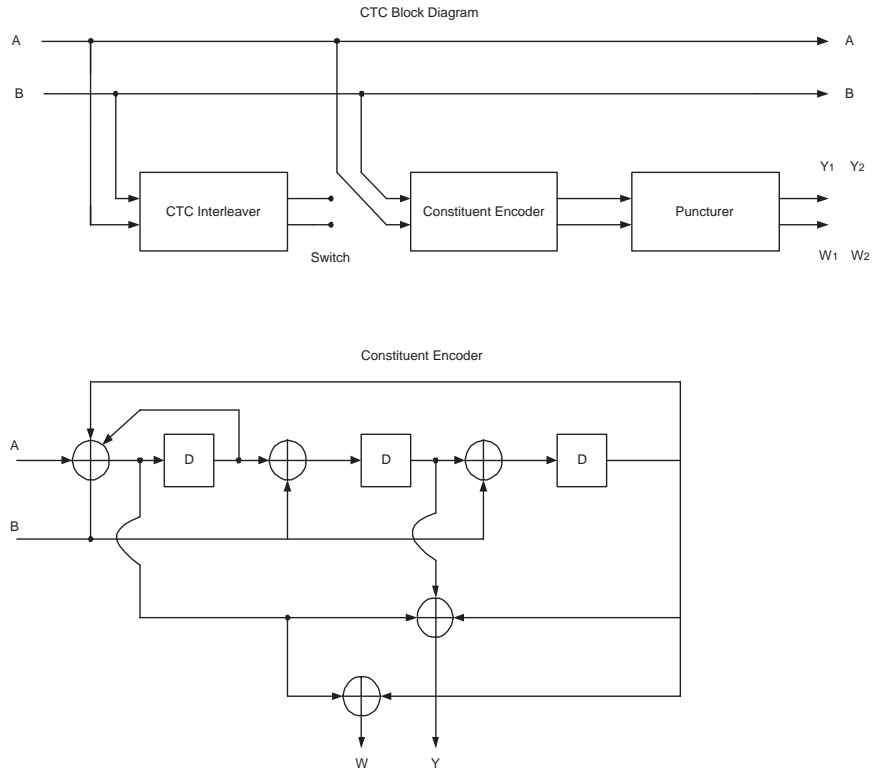


Figure 3.3: CTC encoder.

3.2 Vector Model Implementation of OFDM

The relationship between the channel output and the channel input is,

$$\begin{bmatrix} y_{N-1} \\ y_{N-2} \\ \vdots \\ y_0 \end{bmatrix} = \begin{bmatrix} h_0 & h_1 & \cdots & h_\mu & 0 & \cdots & 0 \\ 0 & h_0 & \cdots & h_{\mu-1} & h_\mu & \cdots & 0 \\ \vdots & \vdots & \ddots & \ddots & \ddots & \ddots & \vdots \\ 0 & \cdots & 0 & h_0 & \cdots & h_{\mu-1} & h_\mu \end{bmatrix} \begin{bmatrix} x_{N-1} \\ \vdots \\ x_0 \\ x_{-1} \\ \vdots \\ x_{-\mu} \end{bmatrix} + \begin{bmatrix} v_{N-1} \\ v_{N-2} \\ \vdots \\ v_o \end{bmatrix} \quad (3.3)$$

This can also be written as $\mathbf{y} = H\mathbf{x} + \mathbf{v}$. Received symbols which are affected by inter symbol interference (ISI) are removed as they are not needed in the process of recovering the input $x[n]$. When coming to input vector \mathbf{x} , the last μ symbols correspond to cyclic prefix: $x_1 = x_N - 1, x_2 = x_N - 2, \dots, x_{-\mu} = x_n - \mu$. Now above equation (3.1) can be written as,

$$\begin{bmatrix} y_{N-1} \\ y_{N-2} \\ \vdots \\ \vdots \\ \vdots \\ y_0 \end{bmatrix} = \begin{bmatrix} h_0 & h_1 & \cdots & h_\mu & 0 & \cdots & 0 \\ 0 & h_0 & \cdots & h_{\mu-1} & h_\mu & \cdots & 0 \\ \vdots & \vdots & \ddots & \ddots & \ddots & \ddots & \vdots \\ 0 & \cdots & 0 & h_0 & \cdots & h_{\mu-1} & h_\mu \\ \vdots & \vdots & \ddots & \ddots & \ddots & \ddots & \vdots \\ h_2 & h_3 & \cdots & h_{\mu-2} & \cdots & h_0 & h_1 \\ h_1 & h_2 & \cdots & h_{\mu-1} & \cdots & 0 & h_0 \end{bmatrix} \begin{bmatrix} x_{N-1} \\ x_{N-2} \\ \vdots \\ \vdots \\ x_0 \end{bmatrix} + \begin{bmatrix} v_{N-1} \\ v_{N-2} \\ \vdots \\ \vdots \\ v_o \end{bmatrix} \quad (3.4)$$

Equation (3.2) can also be written as $\mathbf{y} = \tilde{H}\mathbf{x} + \mathbf{v}$. Every \mathbf{h} vector created is placed into the circulant matrix \tilde{H} given in equation (3.2). This is a square matrix with dimensions N_{FFT} by N_{FFT} where N_{FFT} is the size of FFT used by the OFDM system which is set to 256 in our simulation. Let Λ denote diagonal matrix containing eigenvalues of \tilde{H} . By using various properties of normal matrix and by applying DFT and IDFT on input $x[n]$ vector model of OFDM is given by equation

$$\mathbf{Y} = \Lambda\mathbf{X} + \mathbf{v}_Q. \quad (3.5)$$

where \mathbf{X} is the FFT of \mathbf{x} , \mathbf{Y} is the FFT of \mathbf{y} , and \mathbf{v}_Q is the additive white noise. The vector \mathbf{X} corresponds to the modulated symbols, which are generated directly in the frequency domain. The efficient way to find diagonal matrix Λ is by taking FFT of any column of \tilde{H} . This is due to the spectral theory of circulant matrices. In circulant matrix every row vector is moved one element to the right with respect to the preceding row vector. They are important as they are diagonalized by DFT and hence are helpful to equations containing them as they can be solved quickly using FFT.

3.3 Benefits and Drawbacks of OFDM

We begin by discussing the benefits of OFDM. As stated previously, OFDM system eliminates inter symbol interference (ISI) and is known for its simple and fast implementation of fast fourier transform (FFT). OFDM uses the concept of frequency diversity. OFDM increases data throughput and is also used for high data rate transmission. OFDM reduces spectral interference and also reduces problems due to multipath. Because of its high spectral efficiency, OFDM is used in wireless communications and in many standards.

We now discuss the drawbacks of OFDM. Orthogonal frequency division multiplexing allows only one user at a time to access the channel. OFDM is sensitive to frequency and phase offset. Finally, the use of a cyclic prefix reduces the energy efficiency of OFDM because the energy consumed by the CP is not used to convey information.

Chapter 4

Simulation Model

In this chapter simulation of OFDM modulation is performed. As mentioned earlier focus is made more specifically on implementation of WirelessMAN-OFDM PHY using 802.16-2004 standard. Topics such as Power Spectral Density and rms delay spread are also covered in this chapter.

4.1 OFDM Symbol Parameters

According to our simulation, OFDM is implemented in frequency domain. N_{FFT} gives the total number of subcarriers which is fixed to 256 in our simulation. According to the standard, out of these 256 subcarriers, 200 are used and remaining 56 are unused. Allocation of these 256 subcarriers is shown in Fig. 4.1. The simulation of OFDM modulation is performed in `CmlChannel` function of CML. The symbol vector \mathbf{X} (input to our function) is equal to the length of encoded and modulated CTC code word. \mathbf{X} value depends on number of code bits per frame and varies according to n . For example, consider (48,24) QPSK modulation $n = 48$ bytes. There will be $(48 * 8)/2 = 192$ QPSK symbols and hence length of $\mathbf{X} = 192$. When considering the case of (24,12) QPSK modulation $n = 24$ bytes. There will be $(24 * 8/2) = 96$ QPSK symbols. Hence length of \mathbf{X} in this case is 96.

In our implementation, the modulated symbols are multiplied by a vector of fading coefficients “ \mathbf{a} ”. “ \mathbf{a} ” is found by first generating a random impulse response for the channel and then taking the FFT of the impulse response as described under section 3.1 of the

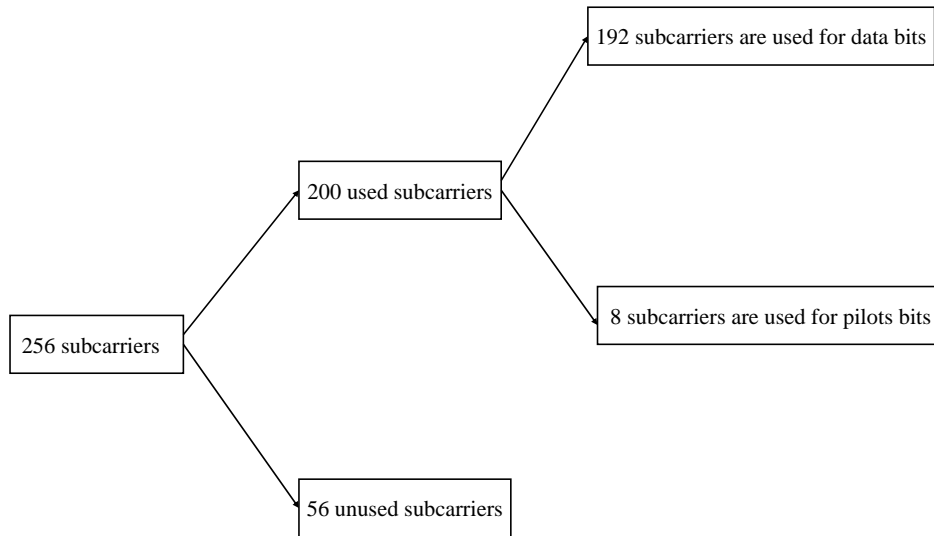


Figure 4.1: Allocation of the 256 subcarriers

chapter 3. Recalling the equation (3.2),

$$\mathbf{Y} = \Lambda \mathbf{X} + \mathbf{v}_Q. \quad (4.1)$$

Modulated vector \mathbf{X} has size 256 but not all 256 are used to convey data.

In order to perform matrix multiplication, vectors \mathbf{a} and \mathbf{X} should be of same size. The vector multiplication can be performed in two ways.

Method 1:

We can lengthen vector \mathbf{X} to equal the size of \mathbf{a} by padding with zeroes in appropriate positions. According to the standard 28 zeros are inserted at the beginning and 27 zeros at the end of the lengthened \mathbf{X} . Also, there will be a zero inserted at the DC level which is the 129th entry of the new lengthened \mathbf{X} . As for the pilots, we can set them to zero but actually they are symbols from signal set. Therefore, $192 + 27(\text{zeros}) + 28(\text{zeros}) + 1(\text{zero}) + 8(\text{pilot bits}) = 256$. Fig. 4.2 describes OFDM subcarriers in frequency domain indicating

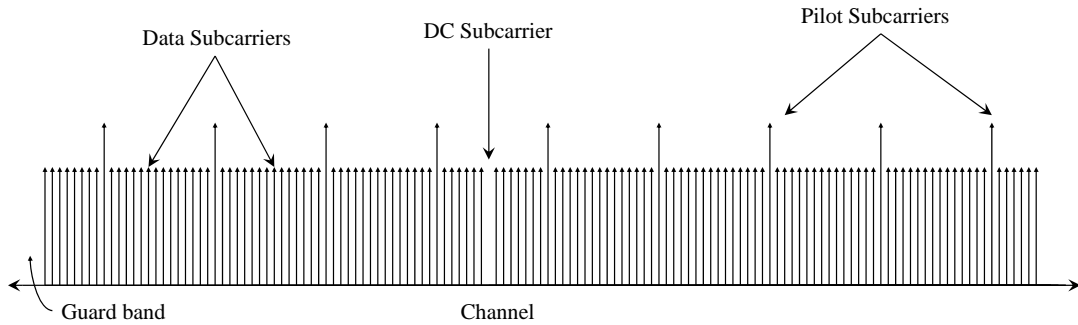


Figure 4.2: OFDM subcarriers in frequency domain

pilot data bits, pilot bits and guard band. In this method \mathbf{X} is forced to be of length 256. Now matrix multiplication can be performed between two vectors of length 256 and then by adding noise, desired output is obtained.

Method 2:

In this method the vector \mathbf{X} is fixed and the vector \mathbf{a} is altered accordingly. The vector \mathbf{X} can be of any length depending on the encoded and modulated CTC code word. Various lengths of \mathbf{X} in our simulation are 192, 96, 48 and 384. The vector \mathbf{a} derived is always of length 256. When the vector \mathbf{X} is of length 192, appropriate pilot and zeros positions of vector \mathbf{a} are stripped out and length of \mathbf{a} is reduced to 192. When the vector \mathbf{X} is of length 96, vector \mathbf{a} is reduced to length 192 as described above and then further reduced to length 96 by taking every alternate value of preciously shortened \mathbf{a} , that is $192/2 = 96$. Similarly when length of the vector \mathbf{X} is 48, same procedure is followed except for taking every fourth value of shortened \mathbf{a} instead of taking every alternative value, that is $192/4 = 48$. In this simulation, method 2 is followed to obtain a desired output.

4.2 Power Delay Profile (PDP) and RMS Delay Spread

The power delay profile represented as $A_c(\tau)$ is a function of time delay. It represents the average power of the multipath components. The PDP of a channel sampled every T_c seconds is given as,

$$A_c(\tau) = \sum_{n=0}^{\mu} G_n \delta[\tau - nT_c] \quad (4.2)$$

where G_n is the relative power of the n^{th} multipath component and it depends on factors such as channel sample rate T_c and β . Relative power G_n is given by the equations,

$$G_0 = \frac{1 - e^{-T_c/\beta}}{1 - e^{-(\mu+1)T_c/\beta}} \quad (4.3)$$

$$G_n = G_{n-1} e^{-T_c/\beta}. \quad (4.4)$$

The value of T_c and β will depend on the channel bandwidth and the rms delay spread. In our simulation, T_c/β is usually taken as 1/2. For fixed T_c/β (say 1/2), μ is varied according to cyclic prefix length. The PDP used in this model is same as the one used in 802.11a and has exponentially decaying nature. See Fig. 4.3.

The rms delay spread describes the dispersive nature of the channel and is represented as σ_{T_m} . The equation of rms delay spread is given as,

$$\sigma_{T_m} = \sqrt{E[T_m^2] - \mu_{T_m}^2} \quad (4.5)$$

where T_m is random delay spread, μ_{T_m} is the average delay and $E[T_m]$ is the expectation which is given as,

$$E[T_m] = \int \tau P_{T_m}(\tau) d\tau \quad (4.6)$$

$P_{T_m}(\tau)$ is the distribution of random variable T_m and is given as the ratio of PDP to average power as shown.

$$P_{T_m}(\tau) = \frac{A_c(\tau)}{G} \quad (4.7)$$

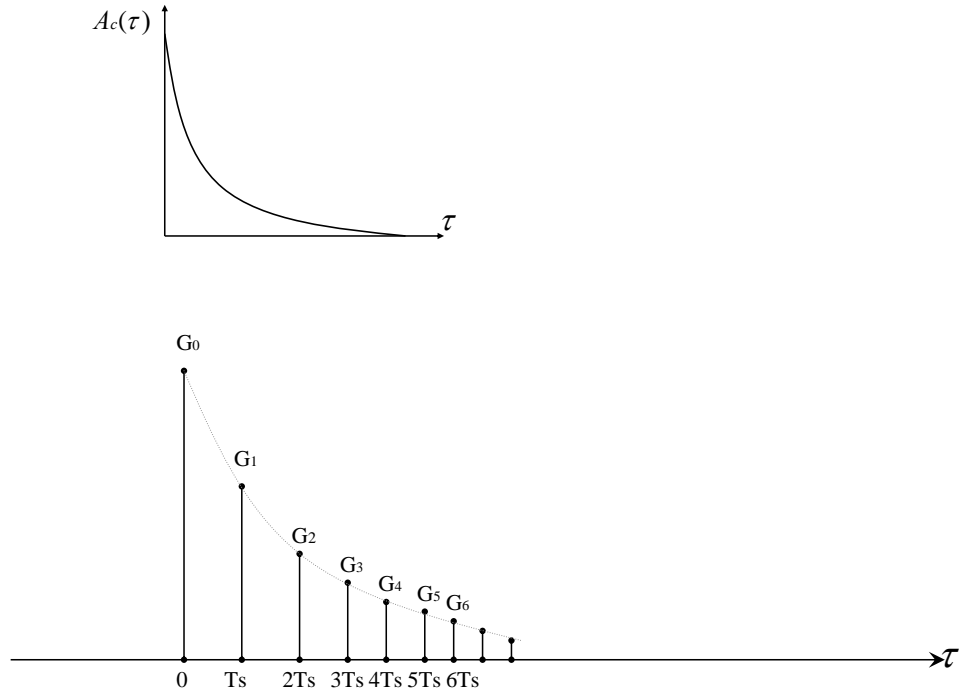


Figure 4.3: Power delay profile as a function of time delay

4.2.1 Relation between rms delay spread, T_c and β

The values T_c and β depend on the channel bandwidth and the rms delay spread σ_{T_m} . Relation between these three parameters are very important in our simulation. The rms delay spread and channel sample rate together can also determine the type of channel fading (flat fading or frequency selective fading). A general relation between the above three parameters is derived here.

$$E[T_m] = \int \tau P_{T_m}(\tau) d\tau \quad (4.8)$$

and

$$E[T_m^k] = \int \tau^k P_{T_m}(\tau) d\tau \quad (4.9)$$

$$= \int \tau^k \frac{A_c(\tau)}{G} d\tau \quad (4.10)$$

$$= \int \tau^k \sum_{n=0}^{\mu} G_n \delta[\tau - nT_c] d\tau \quad (4.11)$$

$$= T_c^k \sum_{n=0}^{\mu} n^k G_n \quad (4.12)$$

For $k = 1, 2$ expectation is calculated and substituted in the equation of rms delay spread.

Now the equation can be written as,

$$\sigma_{T_m} = \sqrt{T_c^2 \left(\sum_{n=0}^{\mu} n^2 G_n - \left(\sum_{n=0}^{\mu} n G_n \right)^2 \right)} \quad (4.13)$$

where

$$G_0 = \frac{1 - e^{-T_c/\beta}}{1 - e^{-(\mu+1)T_c/\beta}} \quad (4.14)$$

$$G_n = G_{n-1} e^{-T_c/\beta} \quad (4.15)$$

When plotting BER for various rms delay spread, T_c/β is varied which in turn varies delay spread. For negligible ISI channel sample rate $T_c \ll \sigma_{T_m}$.

Chapter 5

Results and Conclusion

Various simulations with a variety of modulations (QPSK, 16QAM, and 64QAM) and channel parameters (μ and T_c/β) are tested and their BER and FER are plotted in this chapter. Performance of different modulations are compared for some fixed values of channel parameters.

5.1 Simulation Results

5.1.1 Influence of modulation type

Various specifications considered are:

- FFT size: $N_{FFT} = 256$.
- Channel parameter: $T_c/\beta = 1/2$.
- Modulations compared: QPSK, 16QAM, and 64QAM.
- Code rate: $k/n = 1/2$.
- Bandwidth: $B = 10$ MHz.
- Sampling frequency: $F_s = 28,496$ kHz.
- Subcarrier spacing: $\Delta f = 111$ kHz.

- Length of cyclic prefix: 16 symbols.
- Number of used subcarriers for this simulation is 52 of which 48 are data bits and 4 are pilot bits.

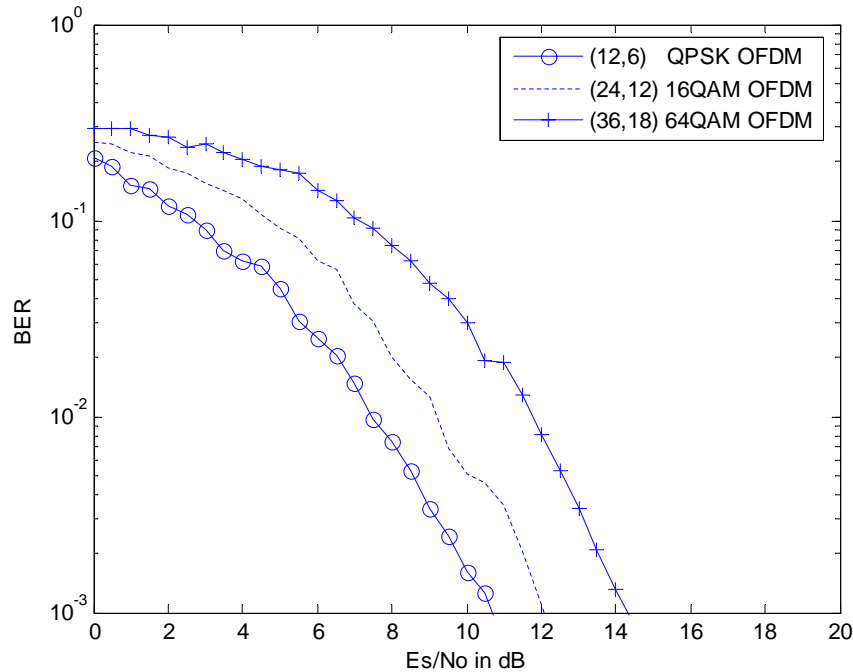


Figure 5.1: BER vs. \mathcal{E}_s/N_0 of various modulations for fixed code rate of $1/2$

Fig. 5.1 shows the bit error rate of various modulations in coded OFDM channel plotted against \mathcal{E}_s/N_0 . When compared QPSK has best performance of all three.

Fig. 5.2 shows the bit error rate of various modulations plotted against \mathcal{E}_b/N_0 . As previously mentioned when plotting BER against \mathcal{E}_b/N_0 there occurs a shift in the \mathcal{E}_b/N_0 axis. The shift depends on number of data bits, cyclic prefix and pilot bits. This shift is due to the loss of energy which accounts due to the use of cyclic prefix and pilots. In this simulation \mathcal{E}_b/N_0 is shifted by $-1.57dB$. From Fig. 5.1 and Fig. 5.2 it can be observed that while QPSK gives the best performance as a function of \mathcal{E}_s/N_0 , 16-QAM actually provides better performance as a function of \mathcal{E}_b/N_0 . The reason for this is most likely because the 16-QAM turbo code is longer than that used by QPSK.

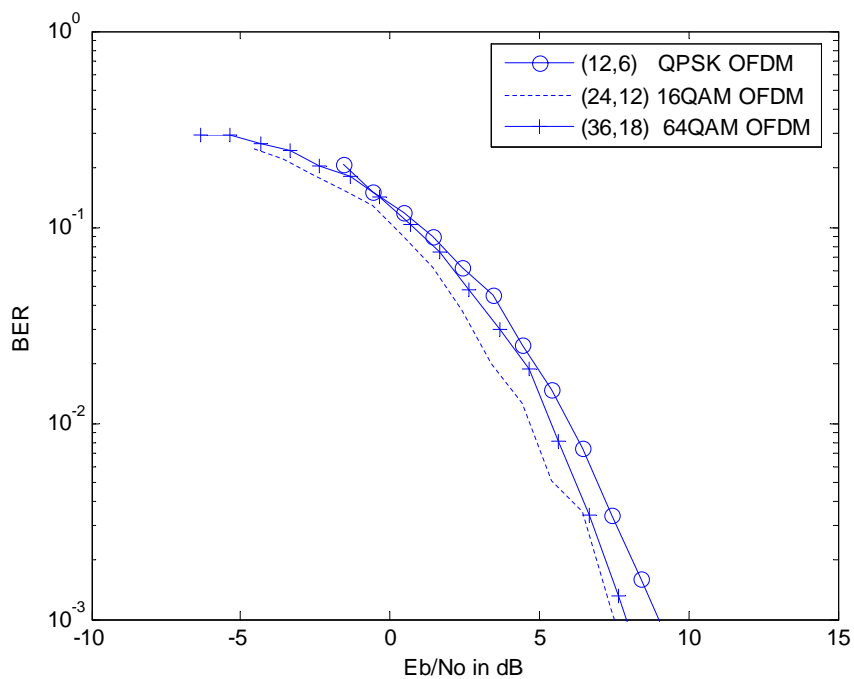


Figure 5.2: BER vs. \mathcal{E}_b/N_0 of various modulations for fixed code rate of 1/2

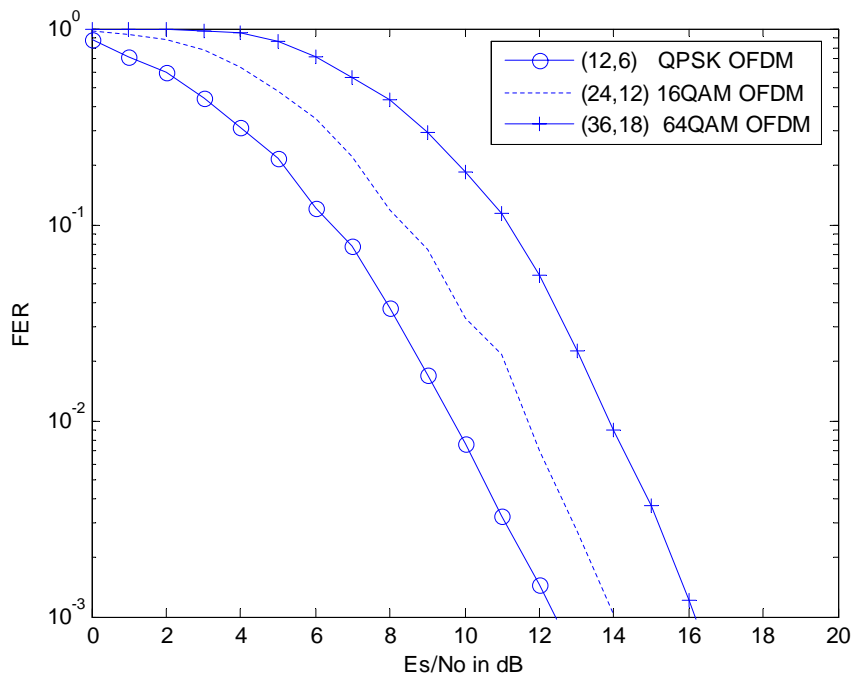


Figure 5.3: FER vs. \mathcal{E}_s/N_0 of various modulations for fixed code rate of 1/2

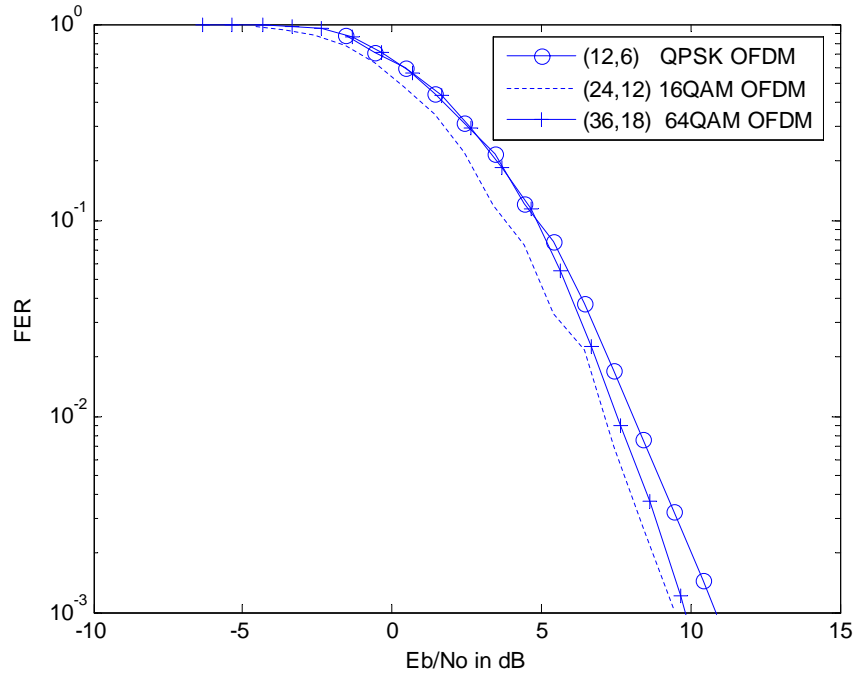


Figure 5.4: FER vs. \mathcal{E}_b/N_0 of various modulations for fixed code rate of 1/2

Using the same specifications specified in section 5.1.1, FER of various modulations for fixed rate 1/2 is plotted. Frame error rate of modulation types QPSK, 16QAM, and 64QAM are plotted against \mathcal{E}_s/N_0 and \mathcal{E}_b/N_0 . Fig. 5.3 and Fig. 5.4 show the comparison of FER for various modulations.

5.1.2 Influence of CTC code rate

In this simulation, modulation is fixed to 64 bit QAM and same specifications specified under section 5.1.1 are used except for the length of cyclic prefix and the rate which are varied. Various code rates considered are 1/2, 2/3, 3/4 and 5/6. See Fig. 5.5. As code rate gets higher, performance degrades. Fig. 5.6 shows BER of 64QAM modulation plotted against \mathcal{E}_b/N_0 .

Frame error rate plotted against \mathcal{E}_s/N_0 and \mathcal{E}_b/N_0 are shown in Fig. 5.7 and Fig. 5.8 respectively.

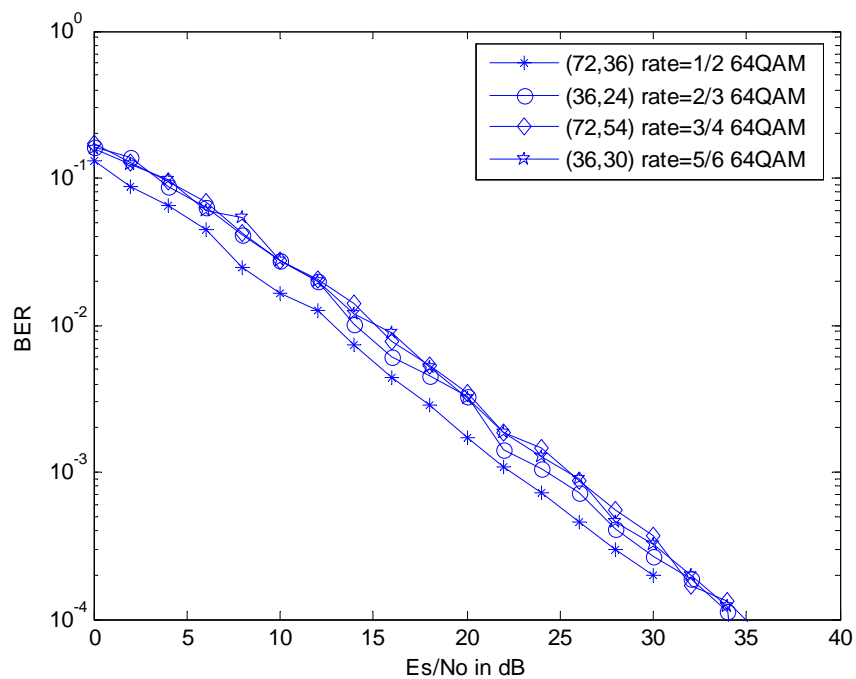


Figure 5.5: BER vs. E_s/N_0 of 64QAM modulation for various code rate

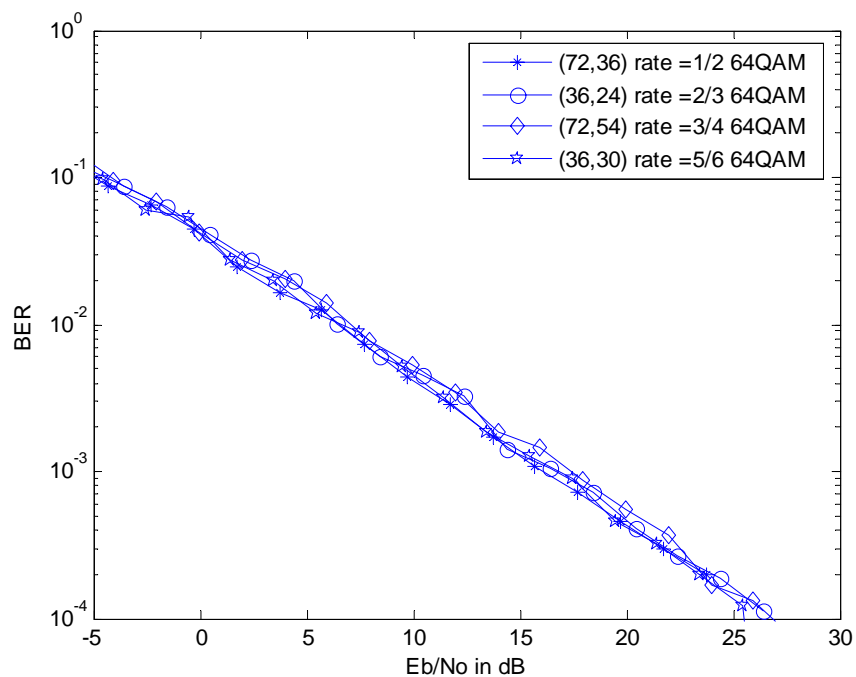


Figure 5.6: BER vs. E_b/N_0 of 64QAM modulation for various code rate

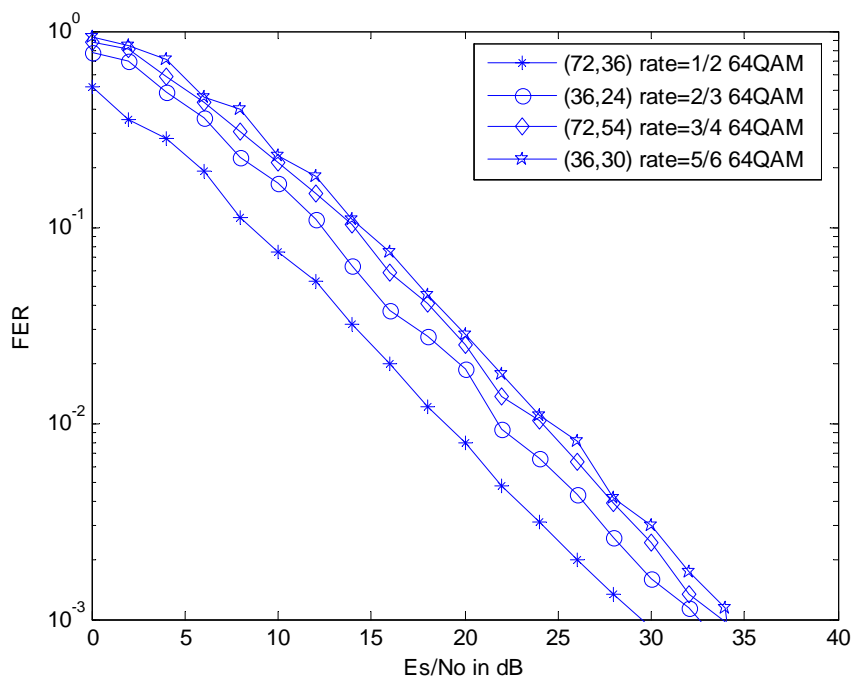


Figure 5.7: FER vs. E_s/N_0 of 64QAM modulation for various code rate

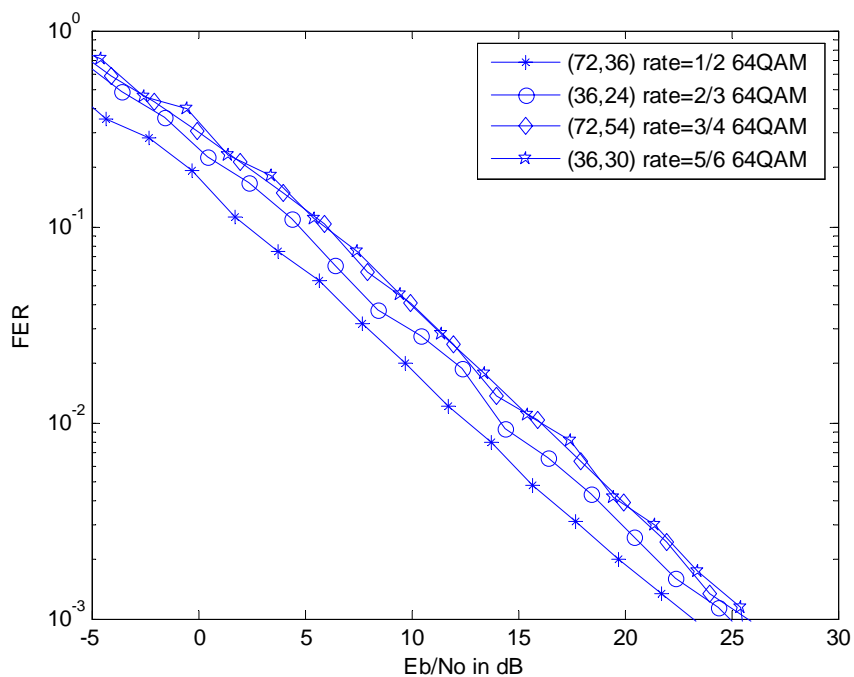


Figure 5.8: FER vs. E_b/N_0 of 64QAM modulation for various code rate

5.1.3 Influence of channel delay spread.

In this simulation, BER of (48,24) QPSK modulation is plotted for various rms delay spread. Channel parameter T_c/β is varied resulting in various rms delay spread values for each T_c/β . Relation between T_c/β and rms delay spread is derived in previous chapter. See section 4.1.1.

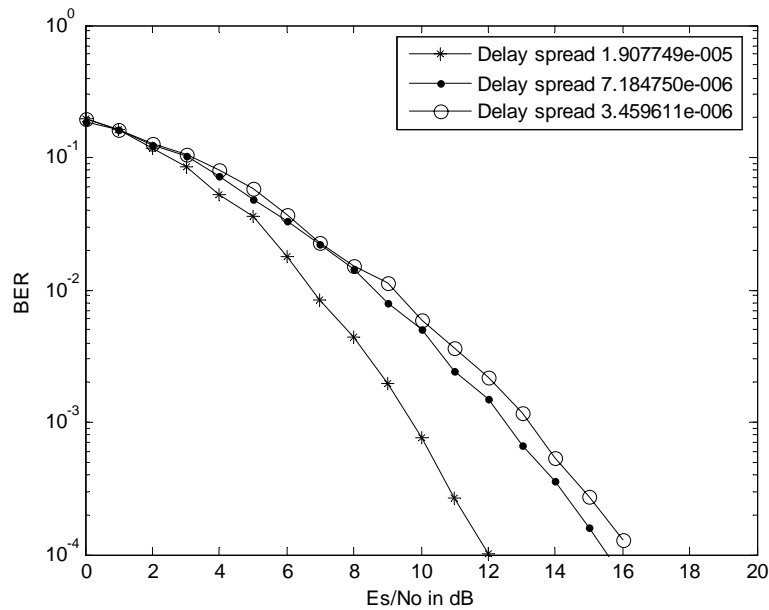


Figure 5.9: BER vs. \mathcal{E}_s/N_0 of (48,24) QPSK modulation for various delay spread

Fig. 5.9 and Fig. 5.10 shows the BER of QPSK modulation for various decreasing rms delay spread plotted against \mathcal{E}_s/N_0 and \mathcal{E}_b/N_0 respectively. As rms delay spread increases, coherent bandwidth decreases and hence frequency diversity increases. This increase in frequency diversity increases the error performance.

From Fig. 5.11 and Fig. 5.12 it can be observed that as rms delay spread increases, performance gets better.

5.2 Conclusion

OFDM which gained popularity for some of its best features such as high spectral efficiency and simple implementation has been used for various wired and wireless applications.

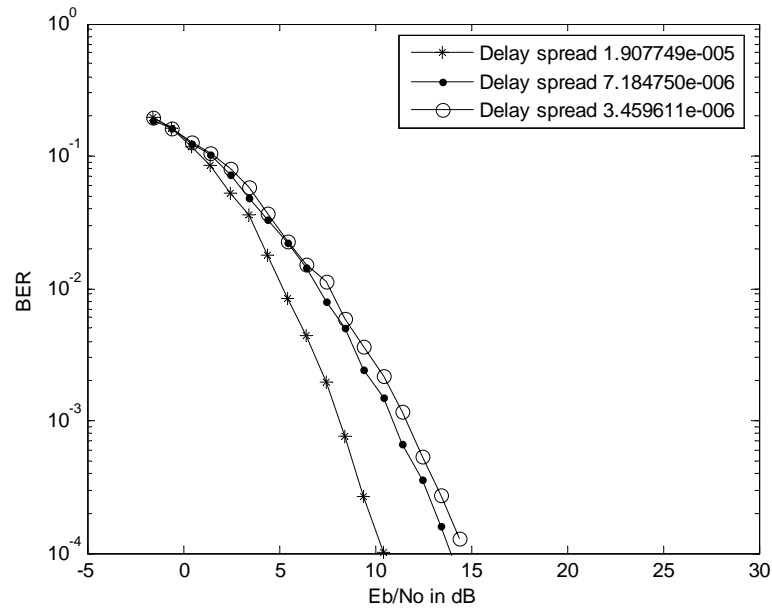


Figure 5.10: BER vs. \mathcal{E}_b/N_0 of (48,24) QPSK modulation for various delay spread

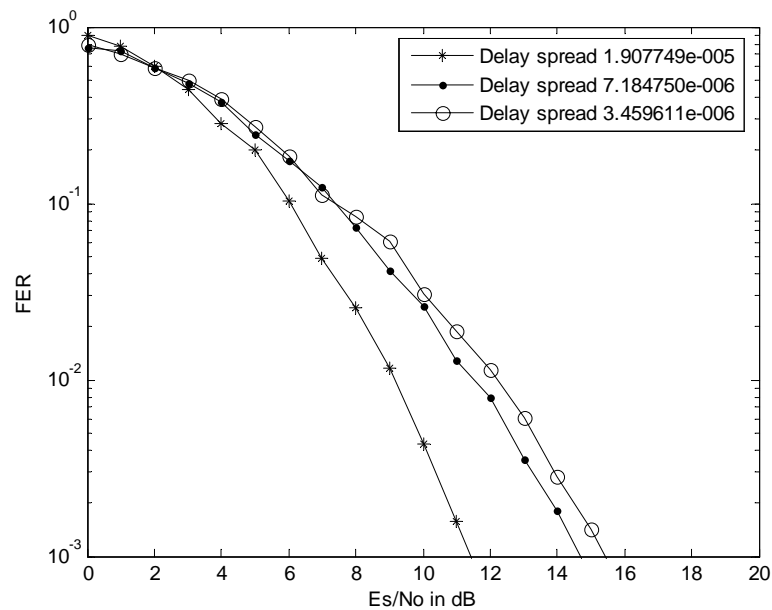


Figure 5.11: FER vs. \mathcal{E}_s/N_0 of (48,24) QPSK modulation for various delay spread

This report has presented a detailed discussion on the implementation of OFDM modulation PHY layer used by the IEEE 802.16 standard. Development of a vector based model for OFDM is the key contribution of this report. Simulations are performed on many modula-

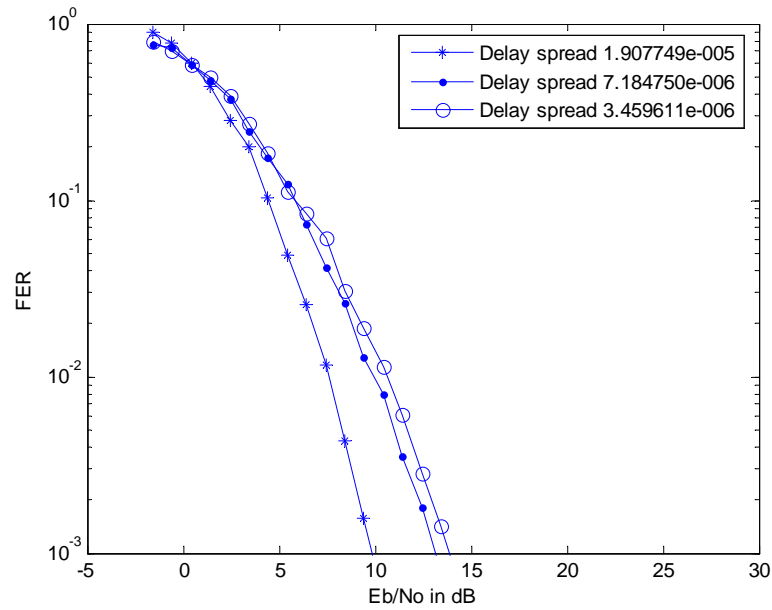


Figure 5.12: FER vs. \mathcal{E}_b/N_0 of (48,24) QPSK modulation for various delay spread

tion schemes successfully and compared for better understanding. Results which included BER and FER plots of various modulations shows the effect of code rate, cyclic- prefix size, modulation order and channel delay spread.

References

- [1] A. Ghosh, D. R. Wolter, J. G. Andrews, and R. Chen, “Broadband wireless access with WiMax/IEEE 802.16:Current performance benchmarks and future potential,” *IEEE Commun. Magazine*, vol. 35, pp. 136–146, Feb 2005.
- [2] D.J. Johnston and M. LaBrecque, “IEEE 802.16 wirelessman specification accelerates wireless broadband access,” *Technology@Intel Magazine*, Aug. 2003.
- [3] Sun, Y., “Bandwidth-efficient wireless OFDM broadband access,” *IEEE Journal*, vol. 19, Iss. 11, Nov. 2001.
- [4] Xiang-Gen Xia, “Precoded OFDM systems robust to spectral null channels and vector OFDM systems with reduced cyclic prefix length” *IEEE International Conference*, vol. 2, June. 2000.
- [5] IEEE Computer Society, and IEEE Microwave Theory and Techniques , *IEEE 802.16-2004 standard for Local and metropolitan area networks. Part 16 : Air Interface for Fixed Broadband Wireless Access Systems*, October 2004.
- [6] Koffman, I. Roman, “Broadband wireless access solutions based on OFDM access in IEEE 802.16,” *IEEE Commun. Magazine*, vol. 40, Iss. 4, pp. 96–103, April 2002.
- [7] A. A. Gilroy and L. G. Kruger, “Broadband internet access: Background and issues,” *CRS Issue Brief for Congress*, Dec. 2003.
- [8] I. Koffman and V. Roman, “Broadband wireless access solutions based on OFDM access in IEEE 802.16,” *IEEE Commun. Magazine*, Vol. 40, pp. 96–103, Apr. 2002.
- [9] Gonzalez-Bayon, Javier, Carreras, Carlos, Fernandez-Herrero, Angel, “A Comparison of Frequency Offset Synchronization Algorithms for WiMAX OFDM Systems,” *International Conference*, Sep 2007.
- [10] A. Zakhia, Y. Peng, and Chang, J.M, “WiMax: The emergence of wireless broadband,” *IT Professional*, vol. 8, pp. 44–48, Jul-Aug 2006.
- [11] Eklund, C.; Marks, R.B.; Stanwood, K.L.; Wang, S., “IEEE Standard 802.16: A Technical Overview of the WirelessMAN Air Interface for Broadband Wireless Access,” *IEEE Commun. Magazine*, vol. 40, Iss. 8, , June. 2002.

- [12] B. Vucetic, and J. Yuan, “Turbo Codes,” *Kluwer Academic Publishers*, 2000.
- [13] Yiqun Ge, Wuxian Shi, Guobin Sun, “A Study of Iterative Joint Synchronization for Time Offset and Frequency Offset in IEEE802.16d WirelessMAN OFDM System,” Conference, Vol. 39, pp. 100–108, Dec. 2005.
- [14] Matthew Valenti, “Wireless communication systems,” Course Notes, WVU, Fall 2007.
- [15] A. Goldsmith, *Wireless Communication*, Cambridge University Press, 2005.
- [16] Matthew C. Valenti, “Iterative Solutions Coded Modulation Library,” January 2008
- [17] J.G. Proakis, *Digital Communications*, 4th ed., New York, NY: McGraw-Hill, 2001.
- [18] C. Berrou, R. Pyndiah, P. Adde, C. Douillard, and R. Le Bidan, “An overview of turbo codes and their applications,” *Wireless Technology.*, Oct. 2005.
- [19] Seong Chul Cho, Jin Up Kim, Kyu Tae Lee and Kyoung Rok Cho, “Convolutional turbo coded OFDM/TDD mobile communication system for high speed multimedia services,” *Telecommunications*, Vol. 40, pp. 244–248, July 2005.
- [20] C. E. Shannon, “A mathematical theory of communication,” *Bell Labs. Tech. Journal*, Part 1 and Part 2, July 1948.